

# Certified Robustness to Adversarial Examples with Differential Privacy

Mathias Lecuyer, Vaggelis Atlidakis, Roxana Geambasu, Daniel Hsu, and Suman Jana  
Columbia University

**Abstract**—Adversarial examples that fool machine learning models, particularly deep neural networks, have been a topic of intense research interest, with attacks and defenses being developed in a tight back-and-forth. Most past defenses are best-effort and have been shown to be vulnerable to sophisticated attacks. Recently a set of *certified defenses* have been introduced, which provide guarantees of robustness to norm-bounded attacks, but they either do not scale to large datasets or are limited in the types of models they can support. This paper presents the first certified defense that both scales to large networks and datasets (such as Google’s Inception network for ImageNet) and applies broadly to arbitrary model types. Our defense is based on a novel connection between robustness against adversarial examples and differential privacy, a cryptographically-inspired technique, that provides a rigorous, generic, and flexible foundation for defense.

## I. Introduction

Deep neural networks (DNNs) perform exceptionally well on many artificial intelligence tasks, including safety- and security-sensitive applications such as self-driving cars [5], malware classification [47], face recognition [46], and critical infrastructure systems [63]. Robustness against malicious attacks is important in many of these applications, yet in recent years it has become increasingly clear that DNNs are extremely vulnerable to a broad range of attacks. Among the possible attacks – broadly surveyed in [45] – are *adversarial examples*: the adversary finds small perturbations to correctly classified inputs that cause a DNN to produce an erroneous prediction, often of the adversary’s choosing [53]. Adversarial examples pose serious threats to security-critical applications. A classic example is an adversary that attaches a small, human-imperceptible sticker onto a stop sign that causes a self-driving car to recognize it as a yield sign. Adversarial examples have also been demonstrated in other domains such as reinforcement learning [33] and generative models [32].

Since the initial demonstration of adversarial examples [53], numerous attacks and defenses have been proposed, each building on one another. Initially, most defenses used *best-effort* approaches and were broken soon after introduction. Model distillation, proposed as a robust defense in [44], was subsequently broken in [7]. Other work [36] claimed that adversarial examples are

unlikely to fool machine learning (ML) models in the real-world due to the rotation and scaling introduced by even slightest camera movements. However, [3] demonstrated a new attack strategy that is robust to rotation and scaling. While this back-and-forth has clearly advanced the state of the art in adversarial ML, recently the community has started to recognize that rigorous, theory-backed, defensive approaches are required to put us off this arms race.

Accordingly, a new set of *certified defenses* have emerged in recent months that provide rigorous guarantees of robustness against norm-bounded attacks [12], [50], [30]. These works alter the learning methods to both optimize for robustness against attack at training time and permit provable robustness checks at inference time using procedures that are customized to the given network architecture. At present, these methods tend to be closely tied to internal network details (e.g., type of activation functions, architecture of the network). They struggle to generalize across different types of DNNs and have only been evaluated on small networks and datasets.

We propose a new and orthogonal approach to certified robustness against adversarial examples that is *broadly applicable, generic, and scalable*. We observe for the first time a connection between *differential privacy* (DP), a cryptography-inspired formalism, and a definition of robustness against norm-based adversarial examples in ML. We leverage this connection to develop *PixelDP*, the first certified defense we are aware of that both scales to large networks and datasets (such as Google’s Inception network trained on ImageNet) and can be adapted broadly to arbitrary DNN architectures. Our approach can even be incorporated without any major changes in the target network (e.g., through a separate auto-encoder as described in Section III-B). We provide a brief overview of our approach below along with the section references where we described the corresponding parts in detail.

§II establishes the DP-robustness connection formally (our first contribution). Note that our approach is orthogonal to differentially private ML algorithms that preserve the privacy of training sets [39], [1], [9] and

have completely different goals, semantic, and algorithms (see Section V for a detailed comparison). To give the intuition, DP is a framework for randomizing computations running on databases such that a small change in the database (removing or altering one row or a small set of rows) is guaranteed to result in a bounded change in the distribution over the algorithm’s outputs. Separately, robustness against adversarial examples can be defined as ensuring that small changes in the input of an ML predictor (such as changing a few pixels in an image in the case of an  $l_0$ -norm attack) will not result in drastic changes to its predictions (such as changing its label from a stop to a yield sign). Thus, if we think of a DNN’s inputs (e.g., images) as databases in DP parlance, and individual features (e.g., pixels) as rows in DP, we observe that randomizing the outputs of a DNN’s prediction function to enforce DP on a small number of pixels in an image *guarantees* robustness of predictions against adversarial examples that can change up to that number of pixels. The connection can be expanded to standard attack norms, including  $l_1$ ,  $l_2$ , and  $l_\infty$  norms.

§III describes *PixelDP*, the first certified defense against norm-based adversarial examples based on differential privacy (our second contribution). A PixelDP DNN incorporates in its architecture a *DP noise layer* that randomizes the network’s computation to enforce DP bounds on how much its predictions can change with small, norm-based changes in the input. At inference time, we leverage the DP bounds to implement a certified robustness check for individual predictions. Passing the check for a given input *guarantees* that no perturbation exists up to a particular size that causes the network to change its prediction. At training time, we incorporate DP noise to give the network an opportunity to optimize its loss function in the context of the inference-time randomization.

§IV presents the first experimental evaluation of a certified adversarial-examples defense for the ImageNet dataset (our third contribution). We additionally evaluate PixelDP on various network architectures for four other datasets (CIFAR-10, CIFAR-100, SVHN, and MNIST), on which previous state-of-the-art defenses – both best effort and certified – are generally evaluated. Our results indicate that PixelDP is (1) as effective at defending against attacks as today’s state-of-the-art best-effort defense and (2) more scalable and broadly applicable compared to any prior certified defense, although not as effective of defending against large attacks as those defenses.

Overall, our experience points to DP as a uniquely generic, broadly applicable, and flexible foundation for certified defense against norm-based adversarial examples (§V). We credit these properties in large part to the *post-processing property of DP*, which lets us incor-

porate the certified defense in a network-agnostic and “slide-in” way. Leveraging this property, we define the first “dataset-level” certified defense against adversarial examples, where the defense can be implemented once for a dataset and subsequently incorporated into any models and tasks using that dataset with only minor modifications (our fourth contribution).

## II. DP-Robustness Connection

This section provides the formal framework for aligning the two concepts: robustness against adversarial examples and differential privacy.

### A. Adversarial ML Background

An ML model can be viewed as a function mapping inputs – typically a vector of numerical feature values – to an output. For multiclass classification tasks, the output is a label from a set of possible labels; for regression tasks, the output is a real number. Focusing on multiclass classification, we define a *model* as a function  $f: \mathbb{R}^n \rightarrow \mathcal{Y}$  that maps  $n$ -dimensional inputs to a label in the set  $\mathcal{Y} = \{1, \dots, Y\}$  of all possible labels. Such models often predict a probability distribution  $(p_1(x), \dots, p_Y(x))$  over the  $Y$  possible labels for a given input  $x$ , and then return the label with highest probability, i.e.,  $f(x) = \arg \max_{y \in \mathcal{Y}} p_y(x)$ .

**Adversarial Examples.** Adversarial examples are a class of attack against ML models, studied particularly on deep neural networks for multiclass image classification. The attacker constructs a small change to a given, fixed input, that wildly changes the predicted output. Notationally, if the input is  $x$ , we denote an adversarial version of that input by  $x + \alpha$ , where  $\alpha$  is the change or perturbation introduced by the attacker. When  $x$  is a vector of pixels (for images), then  $x_i$  is the  $i$ ’th pixel in the image and  $\alpha_i$  is the change to the  $i$ ’th pixel.

It is natural to constrain the amount of change an attacker is allowed to make to the input, and often this is measured by the  $p$ -norm of the change, denoted by  $\|\alpha\|_p$ . For  $1 \leq p < \infty$ , the  $p$ -norm of  $\alpha$  is defined by  $\|\alpha\|_p = (\sum_{i=1}^n |\alpha_i|^p)^{1/p}$ ; for  $p = \infty$ , it is  $\|\alpha\|_\infty = \max_i |\alpha_i|$ . Also commonly used is the 0-norm (which is technically not a norm):  $\|\alpha\|_0 = |\{i : \alpha_i \neq 0\}|$ . A small 0-norm attack is permitted to arbitrarily change a few entries of the input; for example, an attack on the image recognition system for self-driving cars based on putting a sticker in the field of vision is such an attack [18]. Small  $p$ -norm attacks for larger values of  $p$  (including  $p = \infty$ ) require the changes to the pixels to be small in an aggregate sense, but the changes may be spread out over many or all features. A change in the lighting condition of an image may correspond to such an attack [35]. The latter attacks are generally considered more powerful, as they can easily remain invisible to human observers.

Let  $B_p(r) := \{\alpha \in \mathbb{R}^n : \|\alpha\|_p \leq r\}$  be the  $p$ -norm ball of radius  $r$ . For a given classification model,  $f$ , and a fixed input,  $x \in \mathbb{R}^n$ , an attacker is able to craft a successful adversarial example of size  $L$  for a given  $p$ -norm if they find  $\alpha \in B_p(L)$  such that  $f(x + \alpha) \neq f(x)$ . The attacker thus tries to find a small change to  $x$  that will change the predicted label.

**Robustness Definition.** Intuitively, a predictive model may be regarded as robust if its output is insensitive to small changes to any plausible input that may be encountered in deployment. To formalize this notion, we first must establish what qualifies as a plausible input. This is difficult: the literature on adversarial examples has not settled on such a definition. Instead, model insensitivity to input changes is typically assessed on inputs from a test set of data that are not used in model training, and in this work, we adopt this approach.

Next, we must establish a definition for sensitivity to small changes to an input. We say a model  $f$  is insensitive, or *robust*, to attacks of  $p$ -norm  $L$  on a given input  $x$  if  $f(x) = f(x + \alpha)$  for all  $\alpha \in B_p(L)$ . If  $f$  is a multiclass classification model based on label probabilities (as in §II-A), this is equivalent to

$$\forall \alpha \in B_p(L) \cdot p_i(x + \alpha) > \max_{j:j \neq i} p_j(x + \alpha). \quad (1)$$

In other words, a small change in the input does not change which label receives the highest probability.

## B. DP Background

The theory of DP is concerned with whether the output of a computation over a database can reveal information about individual records in the database. To prevent such information leakage, randomness is introduced into the computation so that details of individual records are “hidden” in a certain sense.

A (randomized) algorithm  $A$  that takes as input a database  $d$  (i.e., a set of records, or rows) and outputs a value in a space  $B$  is said to satisfy  $(\epsilon, \delta)$ -DP with respect to a metric  $\rho$  over databases if, for any databases  $d$  and  $d'$  with  $\rho(d, d') \leq 1$ , and for any subset of possible outputs  $S \subseteq B$ , we have

$$P(A(d) \in S) \leq e^\epsilon P(A(d') \in S) + \delta. \quad (2)$$

Here,  $\epsilon > 0$  and  $\delta \in [0, 1]$  are parameters that quantify the strength of the privacy guarantee. In the standard definition of DP, the metric  $\rho$  is the Hamming metric, which simply counts the number of entries that differ in the two databases. For small values of  $\epsilon$  and  $\delta$ , the standard  $(\epsilon, \delta)$ -DP guarantee implies that changing a single entry in the database cannot change the output distribution very much. DP also applies to general metrics  $\rho$  [8], including  $p$ -norms relevant to norm-based adversarial example attacks.

A crucial property of DP, which our defense uses profusely, is the *post-processing guarantee* [17]: any computation applied on the output of an  $(\epsilon, \delta)$ -DP randomized algorithm remains  $(\epsilon, \delta)$ -DP.

## C. DP-Robustness Connection

The intuition behind using DP to provide robustness to adversarial examples is to create a *DP prediction algorithm* such that, given an input example, the predictions are DP with regards to the features of the input (e.g. the pixel of an image to label). In this setting, Equations 1 and 2 provide a link between DP and robustness to adversarial examples.

Regard the feature values (e.g., pixels) of an input  $x$  as the records in a database, and regard  $(p_1(x), \dots, p_Y(x))$  as the probability distribution for the output of a randomized algorithm  $A$  on input  $x$  with range  $\mathcal{Y}$ .<sup>1</sup> Now, we say that  $A$  is an  $(\epsilon, \delta)$ -pixel-level differentially private (or  $(\epsilon, \delta)$ -PixelDP) model if it satisfies  $(\epsilon, \delta)$ -DP (for a given metric). This is formally equivalent to the standard definition of DP, but we use this terminology to emphasize the context in which we apply the definition, which is fundamentally different than the context in which DP is traditionally applied in ML (see §V for distinction).

**Proposition 1.** Suppose  $A$  satisfies  $(\epsilon, \delta)$ -PixelDP with respect to a  $p$ -norm metric, and let  $p_j(x) = P(A(x) = j)$  for each  $j \in \mathcal{Y}$ . For any input  $x$ , if for some  $i \in \mathcal{Y}$ ,

$$p_i(x) > e^{2\epsilon} \max_{j:j \neq i} p_j(x) + (1 + e^\epsilon)\delta,$$

then the multiclass classification model based on label probabilities  $(p_1(x), \dots, p_Y(x))$  is robust to attacks of size  $\|\alpha\|_p \leq 1$  on input  $x$ .

*Proof.* Consider any  $\alpha \in B_p(1)$ , and let  $x' := x + \alpha$ . From Equation (2), we have

$$\begin{aligned} P(A(x) = i) &\leq e^\epsilon P(A(x') = i) + \delta, \\ P(A(x') = j) &\leq e^\epsilon P(A(x) = j) + \delta, \quad j \neq i. \end{aligned}$$

From the first inequality, we obtain a lower-bound on  $p_i(x')$ , and from the second inequality, we obtain an upper-bound on  $\max_{j:j \neq i} p_j(x')$ . The hypothesis in the proposition statement implies that the lower-bound is higher than the upper-bound, which in turn implies the condition from Equation (1) for robustness at  $x$ .  $\square$

The preceding proposition generalizes to attacks of  $p$ -norm size  $L$ , i.e., when  $\|\alpha\|_p \leq L$ , by applying group privacy [17] (see §III-B).

## III. PixelDP Certified Defense

Based on the preceding connection, we develop the *PixelDP certified defense*, a generic and broadly applicable strategy to both increase the robustness of ML

<sup>1</sup>The probabilities  $p_i(x)$  themselves may also be determined using additional randomness.

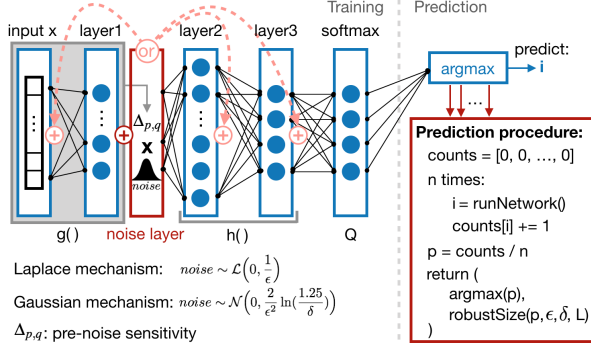


Fig. 1: **PixelDP architecture.** In blue, the original DNN. In red, the noise layer that provides the  $(\epsilon, \delta)$ -DP guarantees. The noise can be added to the inputs *or* any of the following layers, but the distribution is rescaled by the sensitivity  $\Delta_{p,q}$  of the computation performed by each layer before the noise layer. Predictions use multiple noise draws to measure the noise-induced probability distribution over labels.

models and provide certified lower bounds of their accuracy under adversarial attack on a testing set. PixelDP uses DP techniques to ensure that a learned model is not (very) sensitive to small changes in the input. Fig. 1 shows an example three-layer DNN architecture (original network shown in blue) and the changes introduced to the network under the PixelDP strategy (changes shown in red). The changes can be summarized as: (1) introduction of a *noise layer*, which randomizes the DNN to enforce  $(\epsilon, \delta)$ -PixelDP, (2) change of the *training procedure* to account for the added noise, and (2) changes to the *prediction procedure* to provide a certified robustness test.

## A. Overview

A DNN defines a deterministic map  $Q$  from images  $x$  to a probability distribution over the  $Y$  labels  $Q(x) = (Q_1(x), \dots, Q_Y(x))$ . PixelDP adds noise to the DNN to turn  $Q$  into a randomized mechanism  $A_Q$  that, upon input  $x$ , returns a random label  $i \sim Q(x)$  (where the randomness comes from the added noise). If arbitrary randomization is applied, then the mechanism  $A_Q$  may remain as sensitive to small input changes as  $Q$ . To reduce this sensitivity, PixelDP alters the computation of the initial layers of the DNN to satisfy  $(\epsilon, \delta)$ -PixelDP (with respect to  $p$ -norm). We can regard subsequent computation after this randomized DP computation as *post processing* of its output, which preserves the DP guarantees thanks to the post-processing property of DP.

Suppose  $Q(x) = (h_1(g(x)), \dots, h_Y(g(x)))$ , where  $g$  is the computation of some number of initial layers of the DNN (just one in Fig. 1), and for each label  $i \in \{1, \dots, Y\}$ ,  $h_i$  is the subsequent computation that produces  $Q_i(x)$  (the second layer and beyond in Fig. 1). We replace  $g$  with a randomized function  $\tilde{g}$  that satisfies  $(\epsilon, \delta)$ -PixelDP. Concretely, we achieve this

by introducing a *noise layer* (shown in red in Fig. 1) that adds zero-mean noise to the output of  $g$  with standard deviation proportional to the sensitivity  $\Delta$  of  $g$  (i.e., the preceding layers, the grey box in Fig. 1). Now, we obtain a new randomized function  $\tilde{Q}$  via  $\tilde{Q}(x) = (h_1(\tilde{g}(x)), \dots, h_Y(\tilde{g}(x)))$ , which, through the post-processing property of DP [17], also satisfies  $(\epsilon, \delta)$ -PixelDP. The overall randomized mechanism  $A_{\tilde{Q}}$  that returns a random label  $i \sim \tilde{Q}(x)$  upon input  $x$  has the property that small changes to the input image do not change the distribution of the outputted label very much: we have for each  $i = 1, \dots, Y$ ,

$$P(A_{\tilde{Q}}(x+\alpha) = i) \leq e^\epsilon P(A_{\tilde{Q}}(x) = i) + \delta, \quad \alpha \in B_p(1).$$

The resulting PixelDP DNN architecture is non-standard because it is randomized. Nevertheless, we can still train this randomized architecture just as standard DNNs are trained, with a few notable modifications. We describe the new *training procedure* in §III-C.

The robustness properties afforded to our PixelDP DNN architecture concern the probability distribution of its output,  $P(A_{\tilde{Q}}(x) = \cdot)$ , given any input  $x$ . Due to the potentially complex nature of the layers of the DNN following the noise layer, it may be difficult to compute these output probabilities. We therefore resort to Monte Carlo methods to estimate these probabilities at *prediction time*; these probabilities are used to reason about prediction robustness, as shown in §III-D.

## B. DP Noise Layer

The noise layer enforces PixelDP by inserting noise inside the DNN using one of two well-known DP mechanisms: the Laplacian and Gaussian mechanisms. Both rely upon the *sensitivity* of the pre-noise layers (function  $g$ ). The sensitivity of a function  $g$  is defined as the maximum change in output that can be produced by a change in the input, given some distance metrics for the input and output ( $p$ -norm and  $q$ -norm, respectively):

$$\Delta_{p,q} = \Delta_{p,q}^g = \max_{x, x': x \neq x'} \frac{\|g(x) - g(x')\|_q}{\|x - x'\|_p}.$$

Assuming we can compute the sensitivity of the pre-noise layers (addressed shortly), the noise layer leverages the Laplace and Gaussian mechanisms as follows. On every invocation of the network on an input  $x$  (whether for training or prediction) the noise layer computes  $g(x) + Z$ , where the coordinates  $Z = (Z_1, \dots, Z_m)$  are independent random variables from a noise distribution:

- Laplacian mechanism: Uses Laplace distribution with mean zero and standard deviation  $\sigma = \sqrt{2}\Delta_{p,1}L/\epsilon$ ; it gives  $(\epsilon, 0)$ -DP.
- Gaussian mechanism: Uses Gaussian distribution with mean zero and standard deviation  $\sigma = \sqrt{2 \ln(\frac{1.25}{\delta})}\Delta_{p,2}L/\epsilon$ ; it gives  $(\epsilon, \delta)$ -DP for  $\epsilon \leq 1$ .

Here,  $L$  is the *construction attack bound*, an important parameter of the sensitivity analysis that denotes the size (with  $p$ -norm) of the attack against which the PixelDP network provides  $(\epsilon, \delta)$ -DP. For a fixed noise standard deviation  $\sigma$ , the guarantee degrades gracefully: protecting against attacks twice as big halves the  $\epsilon$  in the DP guarantee ( $L \leftarrow 2L \Rightarrow \epsilon \leftarrow 2\epsilon$ ). This property is often referred as group privacy in the DP literature [17].

As with most applications of DP, the difficult task in designing the PixelDP noise layer is *sensitivity analysis*. In our case, we need to compute the sensitivity  $\Delta_{p,q}$  of the *pre-noise function*,  $g$ . Thanks to the post-processing property of DP [17], the DNN's final output remains  $(\epsilon, \delta)$ -PixelDP as long as the post-noise layers do not have access to pre-noise information (e.g., through skip connections). A number of options exist for where to place the noise layer, each with its own sensitivity analysis strategy. Note that the sensitivity analysis strategies are not closely tied to particular network architectures and can therefore easily be applied on a wide variety of networks.

**Option 1: Noise in Image.** The most straightforward placement of the noise layer is right after the input layer, which is equivalent to adding noise to individual pixels of the image. This case makes sensitivity analysis trivial:  $g$  is the identity function,  $\Delta_{1,1} = 1$ , and  $\Delta_{2,2} = 1$ .

**Option 2: Noise after First Layer.** Another option is to place the noise after the first hidden layer, which is usually simple and standard for many DNNs. For example, in image classification, networks often start with a convolution layer. In other cases, DNNs start with fully connected layer. These linear initial layers can be analyzed and their sensitivity computed as follows.

For linear layers, which consist of a linear operator with matrix form  $W \in \mathbb{R}^{m,n}$ , the sensitivity is the matrix norm, defined as:  $\|W\|_{p,q} = \sup_{x: \|x\|_p \leq 1} \|Wx\|_q$ . Indeed, the definition and linearity of  $W$  directly imply that  $\frac{\|Wx\|_q}{\|x\|_p} \leq \|W\|_{p,q}$ , which means that:

$$\Delta_{p,q} = \|W\|_{p,q} \quad (3)$$

We use the following matrix norms [58]:  $\|W\|_{1,1}$  is the maximum 1-norm of  $W$ 's columns;  $\|W\|_{1,2}$  is the maximum 2-norm of  $W$ 's columns; and  $\|W\|_{2,2}$  is the maximum singular value of  $W$ . For  $\infty$ -norm attacks, we need to bound  $\|W\|_{\infty,1}$  or  $\|W\|_{\infty,2}$ , as our DP mechanisms require  $q \in \{1, 2\}$ . However, tight bounds are computationally hard, so we currently use the following bounds:  $\sqrt{n}\|W\|_{2,2}$  or  $\sqrt{m}\|W\|_{\infty,\infty}$  where  $\|W\|_{\infty,\infty}$  is the maximum 1-norm of  $W$ 's rows. While these bounds are suboptimal and lead results that are not as good as for 1-norm or 2-norm attacks, they allow us to include  $\infty$ -norm attacks in our frameworks. We leave the study of better approximate bounds to future work.

For a convolution layer, which is linear but usually not expressed in matrix form, we reshape the input (e.g. the image) as an  $\mathbb{R}^{nd_{in}}$  vector, where  $n$  is the input size (e.g. number of pixels) and  $d_{in}$  the number of input channels (e.g. 3 for the RGB channels of an image). We write the convolution as an  $\mathbb{R}^{nd_{out} \times nd_{in}}$  matrix where each column has all filter maps corresponding to a given input channel, and zero values. This way, a “column” of a convolution consists of all coefficients in the kernel that correspond to a single input channel. Reshaping the input does not change sensitivity.

**Option 3: Noise Deeper in the Network.** One can consider adding noise later in the network using the fact that when applying two functions in a row  $f(g(x))$  we have:  $\Delta_{p,q}^{(f \circ g)} \leq \Delta_{p,r}^{(g)} \Delta_{r,q}^{(f)}$ . For instance, ReLU has a sensitivity of 1 for  $p, q \in \{1, 2, \infty\}$ , hence a linear layer followed by a ReLU has the same bound on the sensitivity as the linear layer alone. However, we find that this approach for sensitivity analysis is difficult to generalize. Combining bounds in this way leads to looser and looser approximations. Moreover, layers such as batch normalization [26], which are popular in image classification networks, do not appear amenable to such bounds (indeed, they are assumed away by some previous defenses [12]). Thus, our general recommendation is to add the DP noise layer early in the network – where bounding the sensitivity is easy – and taking advantage of DP's post-processing property to carry the sensitivity bound through the end of the network.

**Option 4: Noise in Auto-encoder (Dataset-level Defense).** Pushing this reasoning further, we uncover an interesting placement possibility: adding noise even “before” the DNN, say in a *separately trained auto-encoder*. An auto-encoder is a special form of DNN that is trained to predict its own input instead of a label, essentially the learning the identity function  $f(x) = x$ . Auto-encoders are typically used to de-noise inputs [56], and are thus a good fit for PixelDP. Given an image dataset, we can train a PixelDP auto-encoder using the previously described noise layer options, and stack it before a predictive DNN for the classification. We then fine-tune the predictive DNN by running a few training steps on the combined auto-encoder and DNN. Thanks to the decidedly useful post-processing property of DP, a DNN stacked after the auto-encoder preserves the  $(\epsilon, \delta)$ -PixelDP guarantee.

This approach has two advantages. First, the auto-encoder can be developed independently of the DNN, separating the concerns of learning a good PixelDP model and a good predictive DNN. Second, auto-encoders are usually much smaller than predictive DNNs, and are thus much faster to train. We leverage this property to train the first certified model for the large ImageNet dataset, using an auto-encoder and the *pre-*

*trained* Inception-v3 model, a substantial relief in terms of experimental work (§IV-A).

The autoencoder-based architecture opens the door for a *dataset-level certified defense* against adversarial examples, a brand-new concept that we believe holds substantial promise for future security architectures for ML systems. Imagine a dataset curator trains a PixelDP auto-encoder (or several, for various noise configurations) and releases it (them) together with the dataset. Users of the dataset can leverage the auto-encoder as a certified defense for their own predictive models, regardless of the specific tasks, model types, or learning algorithms used to train those models. The effectiveness of the defense does depend on the predictive model, but the implementation need not. We leave for future work research into constructing good, multi-task PixelDP auto-encoders that will be effective for many predictive tasks, but stress here that this concept is enabled only thanks to the post-processing guarantee that is unique to our defense and not shared by any other certified defense we are aware of.

### C. Training Procedure

PixelDP provides robustness guarantees by making the prediction algorithm DP, and as such the certification procedure only requires adding noise at prediction time. Achieving good certified accuracy however requires accounting for the noise layer during training as well. Indeed, adding a noise layer to a pre-trained DNN causes its accuracy to collapse. We thus include the noise layer during training, and use the same loss function and optimization algorithms, such as stochastic gradient descent (SGD), as the original network. Unless we add noise directly to the image, training with noise raises a new challenge: if left unchecked, the training procedure will tend to scale up the sensitivity of the layers preceding the noise layer, voiding the DP guarantees. To avoid this, we enforce bounds on the pre-noise sensitivity during training.

To force the pre-noise sensitivity to be smaller than a constant (e.g.  $\Delta_{p,q} \leq 1$ ), the technique we use depends on the sensitivity we want to bound (i.e.  $(p, q)$ ). For  $\Delta_{1,1}$ ,  $\Delta_{1,2}$ , or  $\Delta_{\infty,\infty}$ , we normalize the columns, or rows, of linear layers and use the regular optimization process with fixed noise variance. For  $\Delta_{2,2}$ , we run the projection step described in [12] after each gradient step from SGD. This makes the pre-noise layers Parseval tight frames, enforcing  $\Delta_{2,2} = 1$ . For the pre-noise layers, we thus alternate between an SGD step with fixed noise variance, and a projection step. Subsequent layers from the original DNN are left unchanged.

### D. Certified Prediction Procedure

While others have proposed adding some noise (not DP-grade) to the training procedure of a DNN to increase

its robustness against adversarial examples [19], we know of no published work that incorporates noise in the prediction procedure. Yet, incorporating noise in the prediction procedure is the key to achieving formal robustness guarantees in PixelDP.

Fig. 1 shows the PixelDP prediction procedure, which differs from the traditional procedure in two ways. In a typical network, the prediction procedure will run the network on a given input  $x$  *once* to obtain a (deterministic) probability distribution over the labels, and then apply an argmax function to select the label(s)  $i$  with the highest one (or more) probability. In PixelDP, the noise layer induces a new probability distribution over the labels and the prediction procedure changes as follows.

First, for a given input, we base our prediction on *multiple* runs of the network, each with a new draw from the Laplacian/Gaussian noise. The multiple runs are part of a Monte Carlo computation to *empirically estimate* the noise-induced distribution over the labels. Here we stress the fact that contrary to typical DP settings, we are not protecting the pixels' privacy, but using DP to bound the change to the output distribution. It is thus sound to use multiple noise draws to estimate the full output distribution on which the DP guarantees hold. From each run, we use the network's argmax predictions to construct a histogram of how many times the noisy DNN outputs each label, which is our estimate of the noise induced distribution over labels.

Second, we compute error bounds to the histogram to account for measurement error in the Monte Carlo computation. We treat each label as a binomial variable (one label against all), and compute Clopper-Pearson intervals, which are conservative in the sense that they never underestimate the error. We then apply a Bonferroni correction for the number of labels, so that all bounds are valid at the same time. The resulting histogram, denoted  $p$ , accurately estimates the noise-induced label distribution within some confidence interval  $\eta$ , (say 95%).

Third, PixelDP returns both the prediction and a *robustness size certificate*. For this, it implements a *robustness test* (method  $robustSize(p, \epsilon, \delta, L)$  in Fig. 1), which uses DP bounds to compute the maximum attack size  $L_{max}$  (in the DNN's PixelDP  $p$ -norm) against which the prediction is guaranteed to be robust: no attack within this size will be able to change the highest probability. The robustness test is given by the following proposition:

**Proposition 2. (Generalization of Proposition 1)** Suppose  $A$  satisfies  $(\epsilon, \delta)$ -PixelDP with respect to changes of size  $L$  in  $p$ -norm metric, and using the notation from Proposition 1 further let  $p_j^{ub}(x)$  and  $p_j^{lb}(x)$  respectively be the upper and lower bound of  $p_j(x)$  with probability

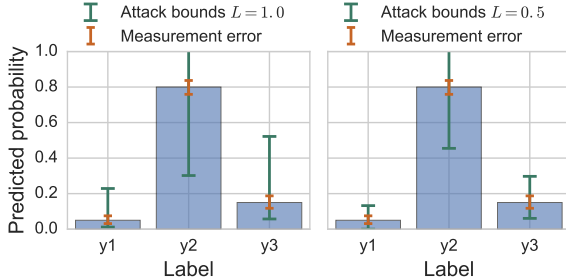


Fig. 2: **Robustness test example.** Histograms the noise-induced label distributions for a  $(1.0, 0.05)$ -PixelDP three-label DNN. Error bars show the measurement error and the DP bounds on adversarial change for: *Left*:  $L = 1.0$ . The prediction is not robust as the lower-bound for the argmax prediction ( $y_2$ ) overlaps the upper-bound of  $y_3$ . *Right*:  $L = 0.5$ . The bounds do not overlap hence prediction is robust.

at least  $\eta$ . For any input  $x$ , if for some  $i \in \mathcal{Y}$ ,

$$p_i^{lb}(x) > e^{2\epsilon} \max_{j:j \neq i} p_j^{ub}(x) + (1 + e^\epsilon)\delta,$$

then the multiclass classification model based on label probabilities  $(p_1(x), \dots, p_Y(x))$  is robust to attacks of  $p$ -norm  $L$  on input  $x$  with probability higher than  $\eta$ .

The proof is similar to the one sketched for Proposition 1 and is detailed in Appendix A. Note that the DP bounds are not probabilistic, and that  $\eta$  comes from the Monte Carlo estimate of  $p$ . We can make  $\eta$  arbitrarily small by using more draws in the estimate.

Recall from III-B that the DP mechanisms have a noise standard deviation  $\sigma$  that grows in  $\frac{\Delta_{p,q}L}{\epsilon}$ . For a given  $\sigma$  used at prediction time, we can solve for the maximum  $L$  for which Proposition 2 is verified:  $L_{max} = \max_{L \in \mathbb{R}^+} L$  such that  $p_i^{lb} > e^{2\epsilon} p_j^{ub} + (1 + e^\epsilon)\delta$  and either  $\sigma = \Delta_{p,1}L/\epsilon$  and  $\delta = 0$  (for Laplace), or  $\sigma = \sqrt{2 \ln(1.25/\delta)} \Delta_{p,2}L/\epsilon$  and  $\epsilon \leq 1$  (for Gaussian). The prediction is certified robust to all attacks up to size  $L_{max}$ , and our method  $robustSize(p, \epsilon, \delta, L)$  outputs  $L_{max}$ . Fig. 2 illustrates the histograms constructed by the prediction procedure to estimate the  $(\epsilon, \delta)$ -DP label distribution, their corresponding measurement error bars, and the DP bounds of how much an attacker can hope to change the probability of each label by perturbing the input up to a particular attack size. The prediction is not robust to attacks of size  $L = 1$  (left), but is robust for  $L = 0.5$  (right), so the maximum robustness size is in between.

For a prediction to be robust, we thus need both small  $(\epsilon, \delta)$  (high noise), and a high probability on the correct label. Since in practice the probability of the correct label degrades with noise, increasing the noise does not always yield higher robust accuracy, and this trade-off needs to be taken into account when designing a PixelDP DNN.

We envision two ways of using these certified predictions. First, when it makes sense to only take actions

on the subset of robust predictions (eg, a human can intervene for the rest), an application can use PixelDP's certified robustness on each prediction. Second, when all points must be classified, PixelDP gives a bound on the accuracy under attack. Like in regular ML, a testing set is used as a proxy for the accuracy on new examples. We can then certify the minimum under attacks up to a threshold size  $T$ , that we call the *prediction robustness threshold*.  $T$  is an inference-time parameter that can differ from the *construction attack bound* parameter,  $\mathcal{L}$ , that is used to configure the standard deviation of the DP noise added with each training and prediction. In practice the accuracy may be higher, as PixelDP yields a lower bound of the accuracy. In this setting the certification is computed only on the testing set, and we do not need to compute the robustness for each prediction. We only need the highest probability label, which requires less noise draws. §IV-E shows that in practice a few hundreds draws a sufficient to retain a large fraction of the certified predictions, while dozens are enough for simple prediction.

## IV. Evaluation

We evaluate PixelDP by answering four key questions:

- Q1:** How does DP noise affect model accuracy?
- Q2:** What accuracy can PixelDP certify and how does that compare to existing certified defenses?
- Q3:** What accuracy does PixelDP yield under attack and how does that compare to both best-effort and certified defenses?
- Q4:** What is the impact of various PixelDP design choices on accuracy and performance?

We answer these questions by evaluating PixelDP on five standard image classification datasets and networks – both large and small – and comparing it with one prior certified defense [30] and one best-effort defense [37]. §IV-A describes the datasets, prior defenses, and our evaluation methodology; subsequent sections address each question in turn. As highlights, we show that PixelDP provides meaningful certified robustness bounds for reasonable degradation in model accuracy on all datasets and networks. To the best of our knowledge, these include the first meaningful certified bounds for large, complex datasets/networks such as the Inception network on ImageNet and Residual Networks on CIFAR-10. There, PixelDP gives 60% certified accuracy for 2-norm attacks up to 0.1 at the cost of 7.4 and 9.2 percentage-point accuracy degradation, respectively. Comparing PixelDP to the prior certified defense on smaller datasets, we show that PixelDP models tend to give higher accuracy on clean examples and under small attacks (e.g., 92.9% vs. 79.6% accuracy on the SVHN dataset, higher robustness to 2-norm attacks smaller than 0.4), but lower accuracy for larger attacks (e.g., 43%

vs. 53% accuracy on SVHN for 2-norm attacks of 0.7). Comparing PixelDP to the best-effort defense on larger models and datasets, we show that PixelDP matches it both on accuracy (e.g., 88.1% for PixelDP vs. 87.3% on CIFAR-10) and robustness to 2-norm bounded attacks of size up to 0.7.

## A. Methodology

**Datasets.** We evaluate PixelDP on image classification tasks from five public datasets listed in Table I. The datasets are listed in descending order of size and complexity for classification tasks. MNIST [61] consists of greyscale handwritten digits and is the easiest to classify. SVHN [42] contains small, real-world digit images cropped from Google Street View photos of house numbers. CIFAR-10 and CIFAR-100 [34] consist of small color images that are each centered on one object of one of 10 or 100 classes, respectively. ImageNet [13] is a large, production-scale image dataset with over 1 million images spread across 1,000 classes.

**Models: Baselines and PixelDP.** We use existing DNN architectures to train a high-performing baseline model for each dataset. Table I shows the accuracy of the baseline models. We then make each of these networks PixelDP with regards to 1-norm and 2-norm bounded attacks, using the techniques described in §III. We also did rudimentary evaluation of  $\infty$ -norm bounded attacks, which the PixelDP formalism can also support, but our results show clearly that tighter bounds are needed to achieve a practical defense. We leave the development of these bounds, and the evaluation of the  $\infty$ -norm defense for future work.

Table II shows all the PixelDP configurations we developed for evaluation. We plan to release all code and configurations after the paper is peer-reviewed and revised for publication. Since most of this section focuses on models with 2-norm attack bounds, we describe the configurations relevant for those models here.

*ImageNet:* We use as baseline a pre-trained version of Inception-v3 [52] available online in Tensorflow [20]. To make it PixelDP, we use the auto-encoder approach described in §III-B, which does not require a full retraining of Inception and was instrumental in our support of ImageNet. The autoencoder has three convolutional layers and tied encoder/decoder weights. The convolution kernels are  $10 \times 10$ ,  $8 \times 8$ , and  $5 \times 5$ , respectively, use a stride 2, and 32, 32, and 64 filters, respectively. To make the autoencoder PixelDP, we add the DP noise after the first convolution layer. We use the Parseval projection step to bound  $\Delta_{2,2}$ . We then stack the baseline Inception-v3 on the PixelDP auto-encoder and fine-tune it for 20k steps, keeping the autoencoder weights constant.

*CIFAR-10, CIFAR-100, SVHN:* We use the same baseline architecture, a state-of-the-art Residual Network (ResNet) [62]. Specifically we use the Tensorflow im-

plementation of a 28-10 wide ResNet [54], with all the default parameters, including the optimizer and learning rate schedule. To make it PixelDP, we slightly alter the architecture to remove the image standardization step. This step makes sensitivity input dependent, which is harder to deal with in PixelDP. Interestingly, removing this step also increases the baseline’s own accuracy for all three datasets. In this section, we therefore report the accuracy of the changed networks as baselines.

*MNIST:* We train a Convolutional Neural Network (CNN) with two  $5 \times 5$  convolutions, with stride 2, and 32 and 64 filters respectively. The convolutions are followed by a fully connected layer with 1024 nodes and a softmax. As a regularizer we use weight decay with a rate of 0.0002.

**Evaluation Metrics.** We use two accuracy metrics to evaluate PixelDP models: *conventional accuracy* and *certified accuracy*. Conventional accuracy denotes the fraction of a testing set on which a model is correct; it is the standard accuracy metric used to evaluate any DNN, defended or not. Certified accuracy denotes the fraction of the testing set on which a certified model’s predictions are both *correct* and *certified robust* for a given prediction robustness threshold; it has become a standard metric to evaluate models trained with *certified defenses* [31], [50], [15]. We also use *precision on certified examples*, which measures the number of correct predictions exclusively on examples that are certified robust for a given prediction robustness threshold. Formally, the metrics are defined as follows:

- 1) *Conventional accuracy*  $\frac{\sum_{i=1}^n \text{isCorrect}(x_i)}{n}$ , where  $n$  is the testing set size and  $\text{isCorrect}(x_i)$  denotes a function returning 1 if the prediction on test sample  $x_i$  returns the correct label, and 0 otherwise.
- 2) *Certified accuracy*  $\frac{\sum_{i=1}^n (\text{isCorrect}(x_i) \& \text{robustSize}(p_i, \epsilon, \delta, L) \geq T)}{n}$ , where  $\text{robustSize}(p_i, \epsilon, \delta, L)$  returns the certified robustness size, which is then compared to the prediction robustness threshold  $T$ .  $p_i$  is the label histogram corresponding to input  $x_i$ .
- 3) *Precision on certified examples*  $\frac{\sum_{i=1}^n (\text{isCorrect}(x_i) \& \text{robustSize}(p_i, \epsilon, \delta, L) \geq T)}{\sum_{i=1}^n \text{robustSize}(p_i, \epsilon, \delta, L) \geq T}$ .

For  $T = 0$  all predictions are robust, so certified accuracy is equivalent to conventional accuracy. Each time we report  $L$  or  $T$ , we use a  $[0, 1]$  pixel range: for instance a  $T$  with a 2-norm of 0.39 corresponds to size 100 in the  $[0, 255]$  pixel range; an  $\infty$ -norm of 0.031 corresponds to an  $\infty$ -norm of 8 in a  $[0, 255]$  pixel range.

**Attack Methodology.** Certified accuracy – as provided by PixelDP and any other certified defense – constitutes a guaranteed lower-bound on accuracy under *any* norm-bounded attack. However, in many cases, the actual accuracy obtained in practice when faced with a specific attack can be much better. How much better depends

| Dataset        | Image size | Training set size | Testing set size | Target labels | Classifier architecture | Baseline accuracy |
|----------------|------------|-------------------|------------------|---------------|-------------------------|-------------------|
| ImageNet [13]  | 299x299x3  | 1.4M              | 50K              | 1000          | Inception V3            | 77.5%             |
| CIFAR-100 [34] | 32x32x3    | 50K               | 10K              | 100           | ResNet                  | 78.6%             |
| CIFAR-10 [34]  | 32x32x3    | 50K               | 10K              | 10            | ResNet                  | 95.5%             |
| SVHN [42]      | 32x32x3    | 73K               | 26K              | 10            | ResNet                  | 96.3%             |
| MNIST [61]     | 28x28x1    | 60K               | 10K              | 10            | CNN                     | 99.2%             |

TABLE I: **Evaluation datasets and baseline models.** Last column shows the accuracy of the baseline, undefended models. The datasets are sorted based on descending order of scale or complexity.

| $p$ -norm used | DP mechanism | Noise location        | Sensitivity approach  |
|----------------|--------------|-----------------------|-----------------------|
| 1-norm         | Laplace      | Image                 | N/A                   |
| 2-norm         | Gaussian     | Image                 | N/A                   |
| 1-norm         | Laplace      | 1 <sup>st</sup> conv. | $\Delta_{1,1} = 1$    |
| 1-norm         | Gaussian     | 1 <sup>st</sup> conv. | $\Delta_{1,2} = 1$    |
| 2-norm         | Gaussian     | 1 <sup>st</sup> conv. | $\Delta_{2,2} \leq 1$ |
| 1-norm         | Laplace      | Autoencoder           | $\Delta_{1,1} = 1$    |
| 2-norm         | Gaussian     | Autoencoder           | $\Delta_{2,2} \leq 1$ |

TABLE II: **Noise layers in our PixelDP DNNs.** For each DNN, we implement defenses for different attack bound norms, requiring different DP mechanisms. We add noise either on the image or after the first convolution.

on the attack. To evaluate this, we developed the strongest norm-based attack strategy we could based on prior literature and adaptations to our specific defense. We describe the attack below. Our overall evaluation methodology consists of two steps. We first perform an attack on 1,000 randomly picked samples (as is customary in defense evaluation [37]) from the corresponding testing set. We then measure conventional accuracy on the attacked test examples.

As we are interested in the impact of the size  $T$  of the adversarial attack, we use a variant of iterative Projected Gradient Descent (PGD) as described in [37]. We make two modifications to this attack, based on prior literature recommendations. First, since our defense adds noise to DNNs, which will increase the variance of the gradients, we average the gradients over multiple draws of noise at each step of the attack, as recommended in [2]. For each example, we use 10 noise draws, and 100 steps of PGD. Second, we use 15 random restarts: we run the attack multiple times on each testing point  $x$ , each time starting from a different small random perturbation. PGD with random restarts was shown empirically to be a very strong first-order attack [37], and is the attack method used to evaluate all the defenses we compare against. Appendix §D contains lower-level details about our attack configuration.

In recent work, Athalye et al. [2] also note that several heuristic defenses do not ensure the absence of adversarial examples, but merely make them harder to find for attacks using first-order gradients. This obfuscated gradients phenomenon, also referred to as gradient masking [45], [55], makes the defense susceptible to new attacks crafted to circumvent that obfuscation [2]. It is important to remember that PixelDP provides certified accuracy

| Dataset   | Baseline | $L = 0.03$ | $L = 0.1$ | $L = 0.3$ | $L = 1.0$ |
|-----------|----------|------------|-----------|-----------|-----------|
| ImageNet  | 77.5%    | –          | 68.3%     | 57.7%     | 37.7%     |
| CIFAR-10  | 95.5%    | 93.3%      | 88.1%     | 75.9%     | 51.4%     |
| CIFAR-100 | 78.6%    | 73.6%      | 66.4%     | –         | –         |
| SVHN      | 96.3%    | 96.1%      | 92.9%     | 81.32%    | 29.8%     |
| MNIST     | 99.2%    | 99.1%      | 99.1%     | 98.5%     | 78.52%    |

TABLE III: **Impact of PixelDP noise on conventional accuracy.** For each DNN, we show different levels of construction attack size  $L$ . Conventional accuracy degrades with noise level.

bounds that, through virtue of DP, are *guaranteed* to hold regardless of the attack used. Still, following guidelines from [2], we perform three sanity checks to rule out obfuscated gradients in PixelDP. First, when growing  $T$ , the accuracy drops to 0 on all models and datasets. Second, our attack significantly outperforms random sampling. Third, our iterative attack is more powerful than the respective single-step attack.

**Prior Defenses for Comparison.** We use two state-of-art defenses as comparisons. First, we use the empirical defense model provided by the Madry Lab for CIFAR-10 [38]. This model is developed in the context of  $\infty$ -norm attacks and uses an adversarial training strategy to approximately minimize the worst case error under malicious samples [37]. This methodology is best effort and supports no formal notion of robustness for individual predictions, as we do in PixelDP. However, because the Madry model performs better under the latest attacks than any other known best-effort defense (and in fact it is the only one not yet broken by these attacks) [2], it represents a good comparison point for PixelDP.

Second, we compare with another approach for certified robustness against  $\infty$ -norm attacks [30], based on robust optimization. This method does not yet scale to the largest datasets (e.g. ImageNet), or the more complex DNNs (e.g. ResNet, Inception) both for computational reasons and because not all necessary layers are yet supported (e.g. BatchNorm). We thus use their largest released model/dataset, namely a CNN with two convolutions and a 100 nodes fully connected layer for the SVHN dataset, and compare their robustness guarantees with our own networks' robustness guarantees. We call their SVHN CNN model *RobustOpt*.

## B. Impact of Noise (Q1)

*Q1: How does DP noise affect the conventional accuracy of our models?* To answer, for each dataset we train

up to four  $(1.0, 0.05)$ -PixelDP DNN, for construction attack bound  $\mathbb{L} \in \{0.03, 0.1, 0.3, 1\}$ . Higher values of  $L$  correspond to robustness against larger attacks and larger noise standard deviation  $\sigma$ .

Table III shows the conventional accuracy of these networks and highlights two parts of an answer to Q1. First, at fairly low but meaningful construction attack bound (e.g.,  $L = 0.1$ ), all of our DNNs exhibit reasonable accuracy loss – *even on ImageNet*, a dataset on which no guarantees have been made to date! ImageNet: The Inception-v3 model stacked on the PixelDP auto-encoder has an accuracy of 68.3% for  $L = 0.1$ , which is reasonable degradation compared to the baseline of 77.5% for the unprotected network. CIFAR-10: Accuracy goes from 95.5% without defense to 88.1% with the  $L = 0.1$  defense. For comparison, the Madry model has an accuracy of 87.3% on CIFAR-10, slightly lower than our defense. SVHN: our  $L = 0.1$  PixelDP network achieves 92.9% conventional accuracy, down from 96.3% for the unprotected network. For comparison, the  $L = 0.1$  RobustOpt network has a conventional accuracy of 79.6%, although they use a smaller DNN due to the computationally intensive method. MNIST: the  $L = 0.1$  PixelDP CNN remains extremely close to the baseline with 99.1% accuracy.

Second, as expected, constructing the network for larger attacks (higher  $L$ ) progressively degrades accuracy. ImageNet: Increasing  $L$  to 0.3 and then 1.0 drops the accuracy to 57.7% and 37.7% respectively. CIFAR-10: The ResNet with the least noise ( $L = 0.03$ ) reaches 93.3% accuracy, close to the baseline of 95.5%; increasing noise levels ( $L = (0.1, 0.3, 1.0)$ ) yields 88.1%, 75.9%, and 51.4%. Yet, as we show in §IV-D, PixelDP networks trained with fairly low  $\mathbb{L}$  values (such as  $\mathbb{L} = 0.1$ ) already provide meaningful empirical protection against larger attacks.

### C. Certified Accuracy (Q2)

*Q2: What accuracy can PixelDP certify on a test set and how does it compare to other certified defenses?* Fig. 3 shows the certified robust accuracy bounds for ImageNet and CIFAR-10 models, trained with various values of the construction attack bound  $\mathbb{L}$ . The certified accuracy is shown as a function of the prediction robustness threshold,  $T$ . We make two observations. First, PixelDP yields meaningful robust accuracy bounds even on large networks for ImageNet (see Fig. 3(a)), attesting the scalability of our approach. The  $\mathbb{L} = 0.1$  network has a certified accuracy of 59% for attacks smaller than 0.09 in 2-norm. The  $\mathbb{L} = 0.3$  network has a certified accuracy of 40% to attacks up to size 0.2. To the best of our knowledge, PixelDP is the first defense to yield DNNs with certified bounds on accuracy under norm-based attacks on datasets of ImageNet’s size and for large networks like Inception.

Second, PixelDP networks constructed for larger attacks (higher  $\mathbb{L}$ , hence higher noise) tend to yield higher certified accuracy for high thresholds  $T$ . For example, the ResNet on CIFAR-10 (see Fig. 3(b)) constructed with  $L = 0.03$  has the highest robust accuracy up to  $T = 0.03$ , but the ResNet constructed with  $L = 0.1$  becomes better past that threshold. Similarly, the  $L = 0.3$  ResNet has higher robust accuracy than the  $L = 0.1$  ResNet above the 0.11 2-norm prediction robustness threshold.

We ran the same experiments on SVHN, CIFAR-100 and MNIST models but omit the graphs for space reasons. Our main conclusion – that making a DNN more robust (higher  $L$  and higher  $T$ ) hurts conventional and low  $T$  certified accuracy but enhances the quality of its high  $T$  predictions – holds in all cases. SVHN: Our  $L = 0.1$  ResNet has a certified accuracy of 73.2% at  $T = 0.1$ , before dropping to 0 for  $T \geq 0.14$ . For  $L = 0.3$ , the certified accuracy at  $T = 0.1$  is lower at 57.5%, but is still 39.6% at  $T = 0.2$  and 24.5% at  $T = 0.3$ . CIFAR-100: For 2-norm bounded attacks and  $L = 0.3$ , accuracy is only 57.3%, but the certified accuracy is still 35% at  $T = 0.1$ . MNIST: The CNN can handle higher noise levels. For  $L = 0.1$ , robust accuracy remains high until  $T = 0.14$  where it is at 97.2% before dropping to 0. The  $L = 0.3$  CNN has an accuracy of 98.5%, and a longer tail of robust accuracy. At  $T = 0.14$  it is still below the lower noise CNN with an accuracy of 94.4%, but at  $T = 0.35$  it still has 77.7% of robust accuracy.

As far as  $\infty$ -norm attacks are concerned, we acknowledge that the size of the attacks against which our current PixelDP defense can certify accuracy is substantially lower than that of previous certified defenses. Although previous defenses have been demonstrated on MNIST and SVHN only, and for smaller DNNs, they achieve  $\infty$ -norm defenses of  $T_\infty = 0.1$  with robust accuracy 91.6% [31] and 65% [50] on MNIST. On SVHN, [31] uses  $T_\infty = 0.01$ , achieving 59.3% of certified accuracy. Using the crude bounds we have between  $p$ -norms makes comparison difficult. Mapping  $\infty$ -norm bounds in 2-norm gives  $T_2 \geq T_\infty$ , yielding very small bounds. On the other hand, translating 2-norm guarantees into  $\infty$ -norm ones (using that  $\|x\|_2 \leq \sqrt{n}\|x\|_\infty$  with  $n$  the size of the image) would require a 2-norm defense of size  $T_2 = 2.8$  to match the  $T_\infty = 0.1$  bound from MNIST, an order of magnitude higher than what we can achieve. As comparison points, our  $L = 0.3$  CNN has a robust accuracy of 91.6% at  $T = 0.19$  and 65% at  $T = 0.39$ . We make the same observation on SVHN, where we would need a bound at  $T_2 = 0.56$  to match the  $T_\infty = 0.01$  bound, but our ResNet with  $L = 0.1$  reaches a similar robust accuracy as RobustOpt for  $T_2 = 0.13$ . This calls for the design  $\infty$ -norm specific PixelDP mechanisms that could also scale to larger DNNs and datasets.

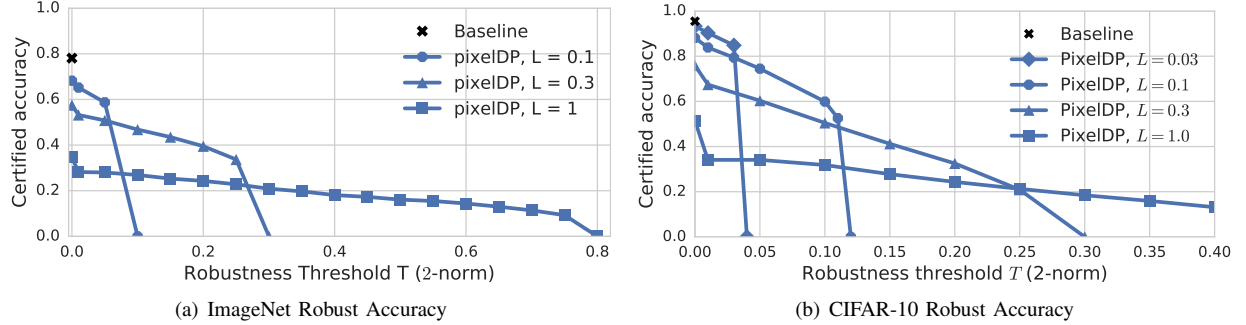


Fig. 3: **Certified accuracy with varying construction attack bound ( $L$ ) and prediction robustness threshold ( $T$ ).** *Config:* ImageNet Inception-v2 plus auto-encoder, CIFAR-10 ResNet, 2-norm bounds. Robust accuracy increases with high-noise networks (high  $L$ ) that are configured to yield more robust predictions (high  $T$ ). Low noise networks are both more accurate and more certifiably robust for low  $T$ .

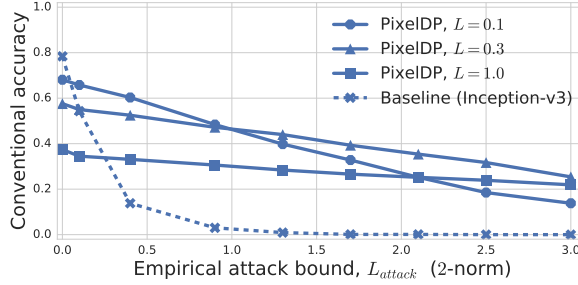


Fig. 4: **Accuracy under attack on ImageNet.** *Config:* ImageNet auto-encoder plus Inception-v3,  $L \in \{0.1, 0.3, 1.0\}$  2-norm attacks. *Concl:* The PixelIDP auto-encoder increases the robustness of Inception-v3 against 2-norm attacks.

Thus, compared to existing certified defenses, PixelIDP provides meaningful certified accuracy bounds for much larger and more complex datasets and networks, but not for as large maximum attack sizes as those defenses. We leave for future work the development of tighter bounds for  $\infty$ -norm defense to certify accuracy under larger attacks.

#### D. Accuracy Under Attack (Q3)

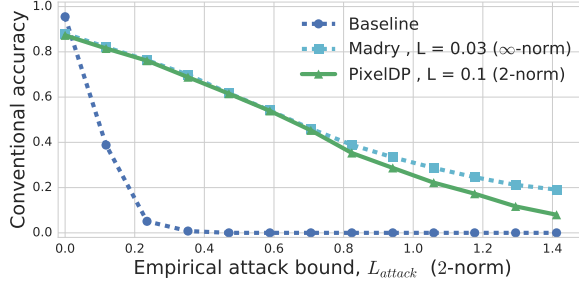
A standard method to evaluate the strength of a defense in this space is to measure the conventional accuracy of a defended model on malicious samples obtained by running a state-of-the-art attack against samples in a held-out testing set [37]. We apply this method to answer three aspects of question *Q3*: (1) *Can PixelIDP help defend complex models on large datasets in practice?* (2) *How does PixelIDP’s accuracy under attack compare to state-of-the-art defenses?* (3) *How does the accuracy under attack change for certified predictions?*

**Accuracy under Attack on ImageNet.** We first study conventional accuracy under attack for PixelIDP models on ImageNet. Fig. 4 shows this metric for 2-norm attacks on the baseline Inception-v3 model, as well as

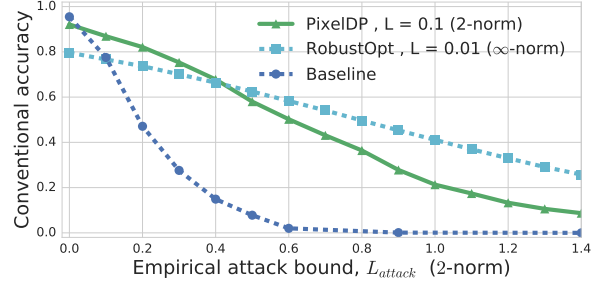
three defended versions, with a stacked PixelIDP auto-encoder trained with construction attack bound  $L \in \{0.1, 0.3, 1.0\}$ . PixelIDP makes the model significantly more robust to attacks. For attacks of size  $L_{\text{attack}} = 0.4$ , the baseline model’s accuracy drops to 14%, which the  $L = 0.1$  PixelIDP is still above 60%. At  $L_{\text{attack}} = 1.5$ , the baseline model has an accuracy of 0, but the  $L = 0.1$  PixelIDP is still at 32%, while the  $L = 0.3$  PixelIDP model have more than 41% accuracy.

**Accuracy under Attack Compared to Madry.** Fig. 5(a) compares conventional accuracy of a PixelIDP model to that of a Madry model, as the empirical attack bound increases for 2-norm attacks. For 2-norm attacks, our model achieves conventional accuracy on par with that of the Madry model for 2-norm attacks up to size 0.7, which corresponds to a 178 2-norm attack in [0-255] pixel range. Both models are dramatically more robust under this attack compared to the baseline (undefended) model. For  $\infty$ -norm attacks our model does not fare as well, which is expected as the PixelIDP model is trained to defend against 2-norm attacks, while the Madry model is optimized for  $\infty$ -norm attacks. For  $L_{\text{attack}} = 0.01$ , PixelIDP’s accuracy is 69%, 8 percentage points lower than Madry’s. The gap increases until PixelIDP arrives at 0 accuracy for  $L_{\text{attack}} = 0.06$ , with Madry still having 22%. Figures appear in Appendix §C.

**Accuracy under Attack Compared to RobustOpt.** Fig. 5(b) shows a similar comparison with the RobustOpt defense [31], that provides certified accuracy bounds for  $\infty$ -norm attacks. The comparison is made on the SVHN dataset, as it has not yet been applied successfully to larger datasets. Due to our use of a larger DNN (ResNet), PixelIDP starts with higher accuracy, which it maintains under attack up to 2-norm 0.4. The RobustOpt then becomes more efficient, beating PixelIDP by a few percentage points at  $L_{\text{attack}} = 0.5$  (62% to 58%), and a full 10 percentage points at  $L_{\text{attack}} = 0.7$  (53% to 43%). We observe the same behavior on  $\infty$ -norm attacks



(a) CIFAR-10



(b) SVHN

Fig. 5: **Accuracy under 2-norm attack for PixelDP vs. Madry and RobustOpt.** *Config:* CIFAR-10 and SVHN models. PixelDP models are trained using 2-norm noise  $L = 0.1$  after the first convolution. Madry model is optimized with adversarial training using PGD for  $\infty$ -norm attacks up to  $L = 0.03$ . RobustOpt use robust optimization against  $\infty$ -norm attacks up to  $L = 0.01$ . *Concl:* For 2-norm attacks, PixelDP is on par with Madry until  $L_{attack} \geq 0.7$ ; RobustOpt has lower accuracy on attacks of size  $L_{attack} \leq 0.4$  but outperforms PixelDP under larger attacks.

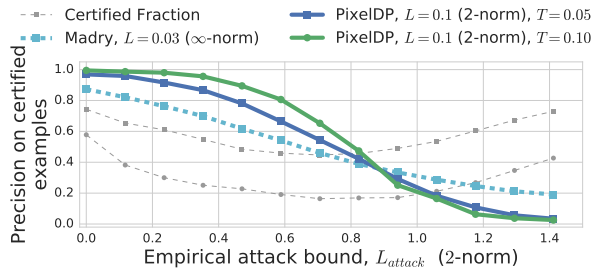


Fig. 6: **PixelDP certified predictions vs. Madry accuracy, under attack.** *Config:* CIFAR-10 ResNets, 2-norm attack. Same models as in Fig. 5. Madry’s robust precision is equivalent to conventional accuracy. *Concl:* PixelDP makes fewer but more correct predictions for up to  $L_{attack} = 0.8$ .

(see Appendix §C): PixelDP has the advantage up to  $L_{attack} = 0.015$  (58.8% to 57.1%), and RobustOpt beats PixelDP thereafter. For instance, at  $L_{attack} = 0.03$ , PixelDP has 22.8% accuracy, to RobustOpt’s 32.7%.

**Precision on Certified Predictions Under Attack.** Another interesting feature of PixelDP is the ability to make certifiably robust predictions. We compute the accuracy of these certified prediction under attack – which we term *robust precision* – and compare them to predictions of the Madry network that do not provide such a certification. Fig. 6 the results for two values of the prediction robustness threshold, and reflect the benefit to be gained by any application that can leverage our theoretical guarantees to filter out non-robust predictions. We observe that PixelDP’s robust predictions are *substantially more correct* than Madry’s predictions up to an empirical attack bound of 0.82. The more conservative the robustness test is (higher  $T$ ), the more correct PixelDP’s predictions are, although it makes fewer of them (Certified Fraction lines). For example, selecting  $T = 0.1$  leads to robust precision

more than 98.1% for attack sizes up to 0.11. This is even higher than the baseline network on benign samples, whose accuracy is 95.1! However, the prediction rate in that case is low (34-55% for the same attack size interval). For less conservative robustness thresholds, such as  $T = 0.05$ , PixelDP’s robust predictions are still more correct than Madry’s predictions (9-21 percentage points more correct up to a 2-bound attack size of 0.82), and can retain a much more meaningful fraction of the predictions (55-73%) for the same attack size interval.

Thus, for applications that can afford to not act on a minority of the predictions, PixelDP’s robust predictions under 2-norm attack are substantially more precise than Madry’s. For applications that need to act on every prediction, PixelDP offers on-par accuracy under 2-norm attack to Madry’s. Interestingly, although our defense is trained for 2-norm attacks, the first conclusion still holds for  $\infty$ -norm attacks; the second (as we saw) does not.

#### E. Design Choices (Q4)

*Q4: What is the impact of various design choices on accuracy and performance?* We study two aspects: (1) the impact of the choice of noise layer positioning on certified accuracy and (2) the computational and performance overhead of the noise layer on prediction and training.

**Noise in Image vs. After First Layer.** We show the impact of the noise layer placement. Fig. 7(a) shows that adding noise after the first convolution, as opposed to directly into the image, gives a slightly higher conventional accuracy, but at the cost of lower certified accuracy for higher prediction robustness thresholds. The more noise (higher values of  $L$ ), the stronger this tradeoff. For example, for  $L = 0.1$ , adding noise after the first convolution brings conventional accuracy from 85% to 88.1%, but is less certified to attacks with 2-norm bigger than 0.05. For  $L = 0.3$  on the other hand, adding noise

to the image reduces the accuracy from 75.9% to 69.3%, but gives higher certified accuracy for attacks of 2-norm above 0.1, with a 6 percentage points increase at 0.2, and a 10 percentage points one at 0.3. Fig. 7(a) shows that this effect is due to the ResNet making a higher number of certified predictions for a given threshold  $T$ , which results in higher certified accuracy but worse certified precision. Depending on use-case, both designs can be advantageous.

**Number of Draws.** We evaluate PixelDP’s computational overhead for training and prediction. PixelDP adds little overhead for *training*, as the only additions are a random noise tensor and sensitivity computations. On our GPU, the CIFAR-10 ResNet baseline takes on average 0.65s per training step. PixelDP versions take at most 0.66s per training step (1.5% overhead). This represents a significant improvement compared to adversarial training (e.g. Madry) that requires finding good adversarial attacks for each image in the mini-batch at each gradient step, or robust optimization (e.g. RobustOpt) that requires solving a constrained optimization problem at each gradient step. The low training overhead is instrumental to our support of large models and datasets. PixelDP impacts *prediction* more substantially, since it uses multiple noise draws to estimate the probabilities over labels. Making a prediction for a single image with 1 noise draw takes 0.01s on average. Making 10 draws brings it only to 0.02s, but 100 requires 0.13s, and 1000, 1.23s. It is possible to use Hoeffding’s inequality [23] to bound the number of draws necessary to distinguish the highest probability with probability at least  $\eta$ , given the difference between the top two probabilities  $p_{\max} - p_2$ . These bounds can be loose, and we do not know the typical value of  $p_{\max} - p_2$  a priori. Running experiments on our DNNs, we found that 300 draws were often necessary to properly certify a prediction, implying a prediction time of 0.42s seconds, a  $42\times$  overhead. This is parallelizable, but resource consumption is still a problem. To make simple predictions (i.e. distinguish the top label when we need to make a prediction on all examples), 25 draws are enough in practice, reducing the overhead to about  $3\times$ .

## V. Related Work

Enormous amount of related literature exists in the space of adversarial ML and beyond. Overall, our work differs from any prior work in three dimensions. First, we are the first to observe the connection between DP and robustness against adversarial examples in ML. Second, our PixelDP defense, built upon this connection, is the first certified defense shown to be amenable to large datasets, such as ImageNet. Third, the level of genericity and flexibility achieved by PixelDP is unparalleled in the certified defense space. PixelDP is not tied to any

particular network architecture, can be deployed with pre-trained networks with minimal fine-tuning effort, and can even be applied to non-DNN models with an auto-encoder-based architecture. We attribute this enormous flexibility to the post-processing guarantee that no other defense exhibits to our knowledge.

**Prior Work on Attacks.** Since the initial adversarial example attacks on DNNs by Szegedy et al. [53], there has been a flurry of attacks aimed at every new tentative defense mechanism. Attacks have used various norms to quantify an attacker’s ability to perturb an image: the 0-norm [43], 1-norm [28], [7], 2-norm [53], [7], [2], and  $\infty$ -norm [19], [59], [7], [2], [35]. State-of-the-art norm-based attacks are based on the PGD [35] and enhanced with adaptive methods against obfuscated gradient defenses per [2]. That is what we use in this paper’s evaluation. Recently, non-norm attacks have been formalized [51]. Building certified defenses against such attacks is beyond the scope of this paper.

**Best-effort Defenses.** In an arms race with attackers, defenders used multiple heuristics to increase robustness of DNNs, at least empirically. These defenses include model distillation [44], automated detection of adversarial examples [22], [41], [40], application of different input transformations [27], [10], randomization [21], [11], and application of generative models [49], [25], [60]. However, all these best-effort defenses have been broken, sometimes even as soon as a few months after their publication [7], [6], [2].

The only empirical defense that still holds is by Madry et al. [37], which is based on adversarial training [19]. Our evaluation shows that PixelDP’s approach achieves comparable performance to Madry et al.’s approach for 2-norm-based attacks while providing significantly stronger robustness guarantees.

Existing randomization-based defenses, unlike PixelDP, only randomize the training process in an ad hoc manner without controlling the sensitivity or changing the inference process. By contrast, PixelDP draws its guarantees from bounding pre-noise sensitivity and randomizing inference to enforce rigorous DP semantic.

**Certified Defenses and Robustness Evaluations.** PixelDP is closest in spirit to a new wave of certified defenses and robustness evaluation methods that has appeared recently. PixelDP offers two functions: (1) a strategy for learning robust models and (2) a method for evaluating the robustness of these models against adversarial examples. Prior to our work, both of these approaches were explored in the literature as described below. However, none of these approaches, unlike PixelDP, can scale to the state-of-the-art models like Google’s Inception trained on ImageNet while providing rigorous robustness guarantees.

First, several certified defenses modify the neural

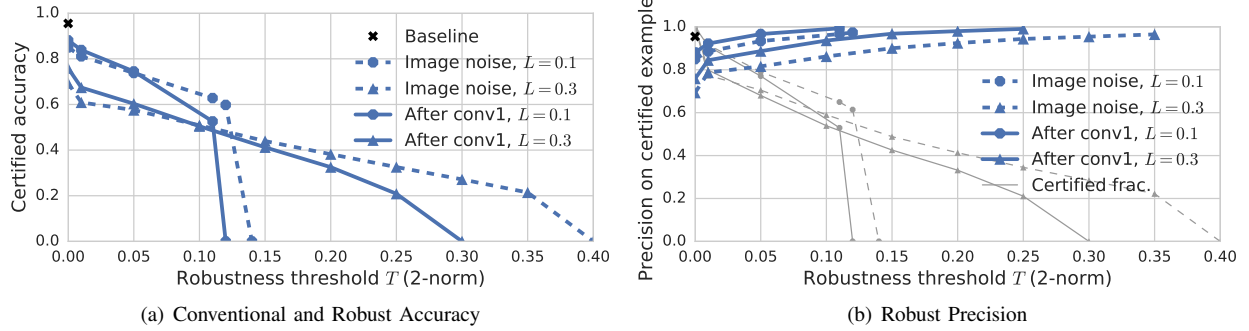


Fig. 7: **Adding noise to the image vs. after the first convolution.** *Config:* CIFAR-10 ResNet, 2-norm bounds. *Concl:* Adding noise after the first convolution is better for low robustness thresholds; adding noise to the image is better for higher thresholds.

network training process to minimize the number of robustness violations [30], [50], [12]. These approaches, though promising, do not yet scale to larger networks like Google Inception [30], [50]. In fact, all published certified defenses have been evaluated on small models and datasets [30], [50], [12], and at least in one case, the authors directly acknowledge that some components of their defense would be “completely infeasible” on ImageNet [30]. Days before this submission, a concurrent paper [15] emerged on arxiv that presents a certified defense evaluated on the CIFAR-10 dataset [34] for multi-layer DNNs (but smaller than ResNets). Their approach is completely different from ours and, based on the current results we see no evidence that it can readily scale to large datasets like ImageNet.

Second, several approaches exist for *formally verifying* the robustness of pre-trained ML models against adversarial attacks, without providing a way to train robust DNNs. These works can be broadly categorized into two classes. One line of work focuses on minimizing false positives by finding concrete counterexamples demonstrating robustness violations [24], [29]. These approaches tend to have very high overhead and struggle to scale to even moderate sized networks. Another line of work focuses on finding conservative bounds on the number of robustness violations [48], [57]. These techniques, while scaling to large networks, cannot provide concrete counterexamples and suffer from high false positive rates.

**Relationship with DP ML Literature.** Significant work has focused on making ML algorithms DP to preserve the privacy of training sets [39], [1], [9]. PixelDP is orthogonal to these approaches, differing in goals, semantic, and algorithms. The only thing we share with DP ML (and most other applied DP literature) are DP theory and mechanisms. The goal of DP ML is to learn the parameters of a model while ensuring DP with respect to the training data. Public release of model parameters

trained using a DP learning algorithm (such as DP empirical risk minimization or ERM) is guaranteed to not reveal much information about individual training examples. PixelDP’s goal is to create a robust predictive model where a small change to any input example does not drastically change the model’s prediction on that example. We achieve this by ensuring that the predictive model is a DP function with respect to the features of an input example (eg, pixels). DP ML algorithms (e.g., DP ERM) do not necessarily produce models that satisfy PixelDP’s semantic, and our training algorithm for producing PixelDP models does not ensure DP of training data.

**Previous DP-Robustness Connections.** Previous work studies generalization properties of DP [4]. It is shown that *learning algorithms* that satisfy DP with respect to the training data have statistical benefits in terms of out-of-sample performance ; or that DP has a deep connection to robustness at the dataset level [14], [16]. Previous work has also shown that DP can be broadened to metrics other than the Hamming distance [8], [14]. Our work is rather different. Our learning algorithm is not DP; rather, the predictor we learn satisfies DP with respect to the atomic units (e.g., pixels) of a given test point.

## VI. Conclusion

We demonstrated a connection between robustness against adversarial examples in machine learning and differential privacy theory. We showed how the connection can be leveraged to develop a certified defense against such attacks that is (1) as effective at defending against 2-norm attacks as today’s state-of-the-art best-effort defense and (2) much more scalable and broadly applicable to large and complex networks compared to any prior certified defense, although not as capable of defending against large attacks. Finally, we presented the first evaluation of a certified 2-norm defense on the large-scale ImageNet dataset. In addition to offer-

ing encouraging results, the evaluation highlighted the substantial flexibility of our approach by leveraging a convenient autoencoder-based architecture to make the experiments possible with limited resources. We leave it for future work to develop tighter bounds to improve the  $\infty$ -norm defense and to develop ways to train PixeIDP auto-encoders that are effective at protecting many downstream models against attack.

## References

- [1] M. Abadi, A. Chu, I. Goodfellow, H. Brendan McMahan, I. Mironov, K. Talwar, and L. Zhang. Deep Learning with Differential Privacy. *ArXiv e-prints*, 2016.
- [2] A. Athalye, N. Carlini, and D. Wagner. Obfuscated gradients give a false sense of security: Circumventing defenses to adversarial examples. 2018.
- [3] A. Athalye and I. Sutskever. Synthesizing robust adversarial examples. *arXiv preprint arXiv:1707.07397*, 2017.
- [4] R. Bassily, K. Nissim, A. Smith, T. Steinke, U. Stemmer, and J. Ullman. Algorithmic stability for adaptive data analysis. In *Proceedings of the forty-eighth annual ACM symposium on Theory of Computing*, 2016.
- [5] M. Bojarski, D. D. Testa, D. Dworakowski, B. Firner, B. Flepp, P. Goyal, L. D. Jackel, M. Monfort, U. Muller, J. Zhang, X. Zhang, J. Zhao, and K. Zieba. End to end learning for self-driving cars. *CoRR*, 2016.
- [6] N. Carlini and D. Wagner. Adversarial examples are not easily detected: Bypassing ten detection methods. In *Proceedings of the 10th ACM Workshop on Artificial Intelligence and Security*, pages 3–14. ACM, 2017.
- [7] N. Carlini and D. A. Wagner. Towards evaluating the robustness of neural networks. In *2017 IEEE Symposium on Security and Privacy, SP 2017, San Jose, CA, USA, May 22–26, 2017*, pages 39–57, 2017.
- [8] K. Chatzikokolakis, M. E. Andrés, N. E. Bordenabe, and C. Palamidessi. Broadening the scope of differential privacy using metrics. In *International Symposium on Privacy Enhancing Technologies Symposium*, 2013.
- [9] K. Chaudhuri, C. Monteleoni, and A. D. Sarwate. Differentially private empirical risk minimization. *J. Mach. Learn. Res.*, 2011.
- [10] Chuan Guo, Mayank Rana, Moustapha Cisse, Laurens van der Maaten. Countering adversarial images using input transformations. *International Conference on Learning Representations*, 2018.
- [11] Cihang Xie, Jianyu Wang, Zhishuai Zhang, Zhou Ren, Alan Yuille. Mitigating adversarial effects through randomization. *International Conference on Learning Representations*, 2018.
- [12] M. Cisse, P. Bojanowski, E. Grave, Y. Dauphin, and N. Usunier. Parseval networks: Improving robustness to adversarial examples. In *Proceedings of the 34th International Conference on Machine Learning*, 2017.
- [13] J. Deng, W. Dong, R. Socher, L.-J. Li, K. Li, and L. Fei-Fei. Imagenet: A large-scale hierarchical image database. In *Computer Vision and Pattern Recognition, 2009. CVPR 2009. IEEE Conference on*, pages 248–255. IEEE, 2009.
- [14] C. Dimitrakakis, B. Nelson, A. Mitrokotsa, and B. Rubinstein. Bayesian Differential Privacy through Posterior Sampling. *arXiv preprint arXiv:1306.1066v5*, 2016.
- [15] K. Dvijotham, S. Gowal, R. Stanforth, R. Arandjelovic, B. O’Donoghue, J. Uesato, and P. Kohli. Training verified learners with learned verifiers. *ArXiv e-prints*, 2018.
- [16] C. Dwork and J. Lei. Differential privacy and robust statistics. In *Proceedings of the forty-first annual ACM symposium on Theory of computing*, 2009.
- [17] C. Dwork, A. Roth, et al. The algorithmic foundations of differential privacy. *Foundations and Trends® in Theoretical Computer Science*, 2014.
- [18] I. Evtimov, K. Eykholt, E. Fernandes, T. Kohno, B. Li, A. Prakash, A. Rahmati, and D. Song. Robust physical world attacks on machine learning models. *arXiv preprint arXiv:1707.08945*, 2017.
- [19] I. Goodfellow, J. Shlens, and C. Szegedy. Explaining and harnessing adversarial examples. In *Proceedings of the 3rd ICLR*, 2015.
- [20] Google. Inception v3. <https://github.com/tensorflow/models/tree/master/research/inception>. Accessed: 2018.
- [21] Guneet S. Dhillon, Kamyar Azizzadenesheli, Jeremy D. Bernstein, Jean Kossaifi, Aran Khanna, Zachary C. Lipton, Aniashree Anandkumar. Stochastic activation pruning for robust adversarial defense. *International Conference on Learning Representations*, 2018.
- [22] D. Hendrycks and K. Gimpel. Early methods for detecting adversarial images. In *ICLR (Workshop Track)*, 2017.
- [23] W. Hoeffding. Probability inequalities for sums of bounded random variables. *Journal of the American statistical association*, 1963.
- [24] X. Huang, M. Kwiatkowska, S. Wang, and M. Wu. Safety verification of deep neural networks. In *Proceedings of the 29th International Conference on Computer Aided Verification*, 2017.
- [25] A. Ilyas, A. Jalal, E. Asteri, C. Daskalakis, and A. G. Dimakis. The robust manifold defense: Adversarial training using generative models. *CoRR*, abs/1712.09196, 2017.
- [26] S. Ioffe and C. Szegedy. Batch normalization: Accelerating deep network training by reducing internal covariate shift. In *International Conference on Machine Learning*, 2015.
- [27] Jacob Buckman, Aurko Roy, Colin Raffel, Ian Goodfellow. Thermometer encoding: One hot way to resist adversarial examples. *International Conference on Learning Representations*, 2018.
- [28] A. Kantchelian, J. Tygar, and A. Joseph. Evasion and hardening of tree ensemble classifiers. In *International Conference on Machine Learning*, 2016.
- [29] G. Katz, C. W. Barrett, D. L. Dill, K. Julian, and M. J. Kochenderfer. Reluplex: An efficient SMT solver for verifying deep neural networks. *CoRR*, 2017.
- [30] J. Z. Kolter and E. Wong. Provable defenses against adversarial examples via the convex outer adversarial polytope. *arXiv preprint arXiv:1711.00851*, 2017.
- [31] J. Z. Kolter and E. Wong. Provable defenses against adversarial examples via the convex outer adversarial polytope. *CoRR*, 2017.
- [32] J. Kos, I. Fischer, and D. Song. Adversarial examples for generative models. *arXiv preprint arXiv:1702.06832*, 2017.
- [33] Kos, Jernej and Song, Dawn. Delving into adversarial attacks on deep policies. *arXiv preprint arXiv:1705.06452*, 2017.
- [34] A. Krizhevsky. Learning multiple layers of features from tiny images. 2009.
- [35] A. Kurakin, I. J. Goodfellow, and S. Bengio. Adversarial examples in the physical world. *arXiv preprint 1607.02533*, 2016.
- [36] J. Lu, H. Sibai, E. Fabry, and D. Forsyth. No need to worry about adversarial examples in object detection in autonomous vehicles. *CVPR*, 2017.
- [37] A. Madry, A. Makelov, L. Schmidt, D. Tsipras, and A. Vladu. Towards deep learning models resistant to adversarial attacks. *CoRR*, abs/1706.06083, 2017.
- [38] Madry Lab. CIFAR-10 Adversarial Examples Challenge. [https://github.com/MadryLab/cifar10\\_challenge](https://github.com/MadryLab/cifar10_challenge). Accessed: 1/22/2017.
- [39] F. McSherry and I. Mironov. Differentially private recommender systems: Building privacy into the netflix prize contenders. In *Proceedings of the 15th ACM SIGKDD International Conference on Knowledge Discovery and Data Mining*, 2009.
- [40] D. Meng and H. Chen. Magnet: A two-pronged defense against adversarial examples. In *CCS*, pages 135–147. ACM, 2017.
- [41] J. H. Metzen, T. Genewein, V. Fischer, and B. Bischoff. On detecting adversarial perturbations. In *Proceedings of the 6th International Conference on Learning Representations*, 2017.
- [42] Y. Netzer, T. Wang, A. Coates, A. Bissacco, B. Wu, and A. Y. Ng. Reading digits in natural images with unsupervised feature learning.
- [43] N. Papernot, P. McDaniel, S. Jha, M. Fredrikson, Z. B. Celik, and A. Swami. The limitations of deep learning in adversarial

settings. In *Proceedings of the 37th IEEE European Symposium on Security and Privacy*, 2016.

[44] N. Papernot, P. McDaniel, X. Wu, S. Jha, and A. Swami. Distillation as a defense to adversarial perturbations against deep neural networks. In *Security and Privacy (SP), 2016 IEEE Symposium on*. IEEE, 2016.

[45] N. Papernot, P. D. McDaniel, A. Sinha, and M. P. Wellman. Towards the science of security and privacy in machine learning. *CoRR*, abs/1611.03814, 2016.

[46] O. M. Parkhi, A. Vedaldi, A. Zisserman, et al. Deep face recognition.

[47] R. Pascanu, J. W. Stokes, H. Sanossian, M. Marinescu, and A. Thomas. Malware classification with recurrent networks. In *Acoustics, Speech and Signal Processing (ICASSP), 2015 IEEE International Conference on*. IEEE, 2015.

[48] J. Peck, J. Roels, B. Goossens, and Y. Saeys. Lower bounds on the robustness to adversarial perturbations. In *Advances in Neural Information Processing Systems*, pages 804–813, 2017.

[49] Pouya Samangouei, Maya Kabkab, Rama Chellappa. Defense-GAN: Protecting classifiers against adversarial attacks using generative models. *International Conference on Learning Representations*, 2018.

[50] A. Raghunathan, J. Steinhardt, and P. Liang. Certified defenses against adversarial examples. *arXiv preprint arXiv:1801.09344*, 2018.

[51] Y. Song, R. Shu, N. Kushman, and S. Ermon. Generative adversarial examples. *arXiv:1805.07894*, 2018.

[52] C. Szegedy, V. Vanhoucke, S. Ioffe, J. Shlens, and Z. Wojna. Rethinking the inception architecture for computer vision. In *Proceedings of the IEEE Conference on Computer Vision and Pattern Recognition*, pages 2818–2826, 2016.

[53] C. Szegedy, W. Zaremba, I. Sutskever, J. Bruna, D. Erhan, I. Goodfellow, and R. Fergus. Intriguing properties of neural networks. In *Proceedings of the 2nd International Conference on Learning Representations*, 2014.

[54] Tensorflow r1.5. Resnet models. <https://github.com/tensorflow/models/tree/r1.5/research/resnet>, 2017.

[55] F. Tramèr, A. Kurakin, N. Papernot, D. Boneh, and P. D. McDaniel. Ensemble adversarial training: Attacks and defenses. *CoRR*, abs/1705.07204, 2017.

[56] P. Vincent, H. Larochelle, I. Lajoie, Y. Bengio, and P.-A. Manzagol. Stacked denoising autoencoders: Learning useful representations in a deep network with a local denoising criterion. *J. Mach. Learn. Res.*, 2010.

[57] T.-W. Weng, H. Zhang, P.-Y. Chen, J. Yi, D. Su, Y. Gao, C.-J. Hsieh, and L. Daniel. Evaluating the robustness of neural networks: An extreme value theory approach. *arXiv preprint arXiv:1801.10578*, 2018.

[58] Wikipedia. Operator norm. [https://en.wikipedia.org/wiki/Operator\\_norm](https://en.wikipedia.org/wiki/Operator_norm), Accessed in 2017.

[59] W. Xu, Y. Qi, and D. Evans. Automatically evading classifiers. In *Proceedings of the 23rd Network and Distributed Systems Symposium*, 2016.

[60] Yang Song, Taesup Kim, Sebastian Nowozin, Stefano Ermon, Nate Kushman. Pixeldefend: Leveraging generative models to understand and defend against adversarial examples. *International Conference on Learning Representations*, 2018.

[61] Yann LeCun, Corinna Cortes, Christopher J.C. Burges. The mnist database of handwritten digits, Accessed in 2017.

[62] S. Zagoruyko and N. Komodakis. Wide residual networks. *CoRR*, 2016.

[63] Z. Zohrevand, U. Glässer, M. A. Tayebi, H. Y. Shahir, M. Shirmaleki, and A. Y. Shahir. Deep learning based forecasting of critical infrastructure data. In *Proceedings of the 2017 ACM on Conference on Information and Knowledge Management, CIKM '17*. ACM, 2017.

## Appendix

### A. Proof of Proposition 2

For convenience we state Proposition 2 again, and write the detailed proof.

**Proposition. (Basic Robustness Test)** Suppose  $A$  satisfies  $(\epsilon, \delta)$ -PixelDP with respect to changes of size  $L$  in  $p$ -norm metric, and using the notation from Proposition 1 further let  $p_j^{ub}(x)$  and  $p_j^{lb}(x)$  respectively be the upper and lower bound interval of  $p_j(x)$ , with probability  $\eta$ . For any input  $x$ , if for some  $i \in \mathcal{Y}$ ,

$$p_i^{lb}(x) > e^{2\epsilon} \max_{j:j \neq i} p_j^{ub}(x) + (1 + e^\epsilon)\delta,$$

then the multiclass classification model based on label probabilities  $(p_1(x), \dots, p_Y(x))$  is robust to attacks of  $p$ -norm  $L$  on input  $x$  with probability higher than  $\eta$ .

*Proof.* Consider any  $\alpha \in B_p(L)$ , and let  $x' := x + \alpha$ . From Equation (2), we have with  $p > \eta$  that

$$\begin{aligned} p_i(x') &\geq (p_i(x) - \delta)/e^\epsilon \geq (p_i^{lb}(x) - \delta)/e^\epsilon, \\ p_{j:j \neq i}(x') &\leq e^\epsilon \max_{j:j \neq i} p_j^{ub}(x) + \delta, \quad j \neq i. \end{aligned}$$

Starting from the first inequality, and using the hypothesis, followed by the second inequality, we get

$$\begin{aligned} p_i^{lb}(x) &> e^{2\epsilon} \max_{j:j \neq i} p_j^{ub}(x) + (1 + e^\epsilon)\delta \Rightarrow \\ p_i(x') &\geq (p_i^{lb}(x) - \delta)/e^\epsilon > e^\epsilon \max_{j:j \neq i} p_j^{ub}(x) + \delta \\ &> p_{j:j \neq i}(x') \end{aligned}$$

which is the robustness condition from Equation (1).  $\square$

This shows that if the bounds computed from the measurement error and differential privacy do not overlap, the prediction is robust to adversarial perturbations in  $B_p(L)$ .

### B. Design Choice: Laplace vs. Gaussian

We study the impact of the DP mechanism used. When training to PixelDP with regards to the 1-norm of the attack, both the Laplace and Gaussian mechanisms can be used after the first convolution, by respectively controlling the  $\Delta_{1,1}$  or  $\Delta_{1,2}$  sensitivity. Fig. 8 shows that for our ResNet, the Laplace mechanism is better suited to low levels of noise: for  $L = 0.1$ , it yields a slightly higher accuracy (90.5% against 88.9%), as well as better robust accuracy with a maximum robustness size of 1-norm 0.22 instead of 0.19, and a robust accuracy of 73% against 65.4% at the 0.19 threshold. On the other hand, when adding more noise (e.g.  $L = 0.3$ ), the Gaussian mechanism performs better than the Laplace mechanism, consistently yielding a robust accuracy 1.5 percentage point higher.

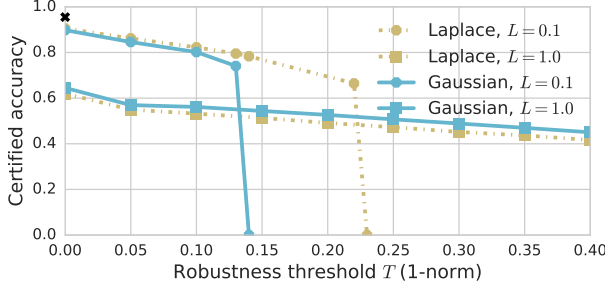


Fig. 8: **Laplace vs. Gaussian.** Robust performance of a ResNet on the CIFAR-10 dataset, for robustness thresholds with regards to 1-norm bounded attacks. The noise standard deviation is computed with  $\epsilon = 1.0$  and construction attack bound  $L$ . The Laplace mechanism yields better accuracy for low noise levels, but the Gaussian mechanism is better for high noise ResNets.

### C. Accuracy Under $L_\infty$ Attacks

We show the PixelDP’s accuracy under  $L_\infty$  attacks, compared to the Madry and RobustOpt models, both trained specifically against this type of attacks. On CIFAR-10, the Madry model outperforms PixelDP: for  $L_{\text{attack}} = 0.01$ , PixelDP’s accuracy is 69%, 8 percentage points lower than Madry’s. The gap increases until PixelDP arrives at 0 accuracy for  $L_{\text{attack}} = 0.06$ , with Madry still having 22%.

On SVHN, against the RobustOpt model, trained with robust optimization against  $L_\infty$  attacks, PixelDP is better up to  $L_\infty = 0.015$ , due to its support of larger ResNet models. For attacks of  $\infty$ -norm above this value, RobustOpt is more robust.

### D. Adaptive PGD Attack Details

We specify a few important but lower level aspects about our attack procedure for both 2-norm and  $\infty$ -norm attacks. We design our attack to use multiple noise draws (*e.g.*, 10 per gradient update) and also to perform random restarts (*e.g.*, 15 for each data point).

*2-norm Attacks:* We perform  $k = 100$  gradient steps and select a step size of  $\frac{2.5L}{k}$  (where  $L$  is the 2-norm size of the attack) divided by the number of gradient steps.

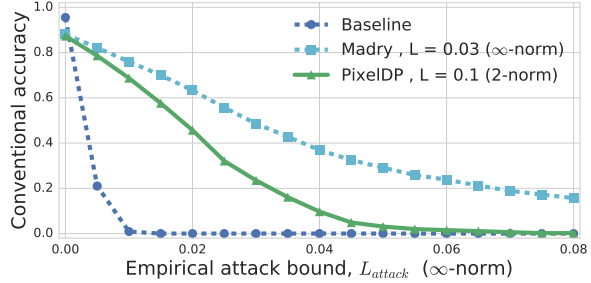


Fig. 9: **Accuracy under  $\infty$ -norm attacks for PixelDP and Madry.** Config: ResNet on the CIFAR-10 dataset. The Madry model, explicitly trained against  $L_\infty$  attacks, outperforms PixelDP. The difference increases with the size of the attack. This heuristic ensures that all feasible points within the 2-norm ball can be reached after 100 steps. After each gradient calculation we normalize the gradient tensor with its 2-norm value to avoid being stuck because of small gradients. After each step, if the attack is larger than the maximum size, we project it on the 2-norm ball by normalizing it (projection phase).

*$\infty$ -norm Attacks:* We perform  $\max(L + 8, 1.5L)$  gradient steps (where  $L$  is the  $\infty$ -norm size of the attack) and maintain a constant step of size 0.003 (which corresponds to the minimum pixel increment in a discrete  $[0, 255]$  pixel range). At the end of each gradient step we clip the size of the perturbation at the granularity of individual pixel values to enforce perturbations within the  $\infty$ -norm ball of the given attack size (projection phase).

For both 2-norm and  $\infty$ -norm attacks, each random restart is started by prepending a small random step before starting PGD iterations. This is an iterative alternative to the randomized single-step attack proposed by Tramèr et al. [55]. To perform the initial random step, we draw noise from a uniform distribution in  $[-0.003, +0.003]$ .